CHEMICAL ENGINEERING TRANSACTIONS
VOL. 47, 2016
A publication of AIDIC
The Italian Association of Chemical Engineering
Online at www.aidic.it/cet
Guest Editors: Angelo Chianese, Luca Di Palma, Elisabetta Petrucci, Marco Stoller

ISBN978-88-95608-38-9; **ISSN** 2283-9216
DOI: 10.3303/CET1647014

Super-Paramagnetic Nanoparticles: Manufacturing, Structure, Properties, Simulation, Applications

Baja Adamaki[a], Despoina Karatza[b], Simeone Chianese[b], Dino Musmarra[b]*, Eleni Metaxa[a], Evangelos Hristoforou[a]

[a]Laboratory of Physical Metallurgy, National Technical University of Athens, Zografou Campus, 15780 Athens, Greece
[b]Dipartimento di Ingegneria Civile, Design, Edilizia e Ambiente, Seconda Università degli Studi di Napoli, Via Roma 9, 81031 Aversa (CE)
dino.musmarra@unina2.it

In this paper, after illustrating the current state of the art, we present our own technology in manufacturing super-paramagnetic nanoparticles (SPAN). The method is based on chemical coprecipitation by using single ion precursors, like chloride or/and nitrate salts. Apart from synthetic route description,a demonstration ofthe methods used for structural analysis and electric-magnetic properties determination is done followed by the comments and remarks on the recorded results. Finally, the role of doping in magnetic and optical properties of the prepared nanomagnetic materials is illustrated and the potential utilization of these materials in varioustechnological applications is presented.

1. Introduction

Spinel ferrites (or ferrospinels) and especially, nanosized ferriteshave attracted considerable attention, since they are multifunctional materials with a wide spectrum of applications, as in magnetic fluids (Chikazumiet al., 1987), magnetic resonance imaging (Mornet et al., 2006), data storage (Hyeon T., 2003), biomedicine technology (Gupta et al., 2005),catalysis (Chistyakovet al., 2013), sensors (Peña and Pierro, 1981), wastewater treatment (Ruzmanovaet al., 2013), microwave devices (Palmaet al.,2013), etc., due to their optical, mechanical, thermal and magnetic properties, which are controlled by the cation distribution between the tetrahedral A-site and octahedral B-site of the spinel structure. The cation distribution depends on the ionic radii of cations, preparation method, preparation conditions, chemical composition, sintering temperature, doping and substitution process (Deraz, 2012). To meet the technological challenges,nano-sized materials with a particular structure, surface and magnetic properties are a great demand.The magnetic properties of the nanosized ferrites are entirely different from those of their bulk counterparts, such as the super paramagnetic behavior and associated properties.
If some of iron cation (Fe3+/Fe2+) sites in the spinel ferrite structure substituted by other metal cations (M3+/M2+), the formation of mixed (0<δ<1) or inverse (δ=1) spinel structure A(1-δ)Bδ[AδB(2-δ)]O4 is generally promoted, where δ is the inversion degree of the spinel sytructuredefined as the fraction of the tetrahedral sites of the spinel occupied by Fe3+ cations.For a normal spinel (AB2O4), δ=0, whereas for an inverse spinel (B[AB]O4, e.g., Fe3O4), δ=1. The physicochemical and magnetic properties of ferrospinels strongly depend on the site, nature and amount of the M-substituent (or dopants) at the A and B sites in the structure of spinel. Spinel ferrites are characterized as ferrimagnetic materials due tothe incomplete compensation of magnetic moments of bivalent iron ions in the two sub-lattices – tetrahedral and octahedral – of the whole crystal lattice of spinel structure. Furthermore, the sizes of ion-dopants can also affect the rate of charge exchange between trivalent and bivalent iron cations (Fe3+− e-↔ Fe2+), which in turn has a great importance in case of adsorption, catalysis and sensor applications of spinel ferrites. In the majority of these applications, such substitutions improve thermal and textural stability on the one hand and on the other hand, they promote reducibility (Fe2O3→ Fe3O4). Transition and inner transition metal substituents (dopants) can be expected to strongly modify the redox properties, namely the charge transfer rate among iron cations. Different metals have different reduction ability to Fe3+.For example, the reduction ability of nickel and

Please cite this article as: Adamaki B., Karatza D., Chianese S., Musmarra D., Metaxa E., Hristoforou E., 2016, Super-paramagnetic nanoparticles: manufacturing, structure, properties, simulation, applications, Chemical Engineering Transactions, 47, 79-84
DOI: 10.3303/CET1647014

zinc−expessed as “oxygen deficiency value” of the doped magnetite − reported as 0.19 and 0.06 by Kodama et al. (1995), while 0.58 and 0.16 by Nordhei et al. (2009), respectively. This value is much higher for nickel metal as it has 3d8 orbital while zinc has 3d10(Kodama et al., 1995).Additionally, the effect of non-magnetic metal transition dopants with similar ionic radii with iron cations, on the magnetic properties of doping magnetite show, for example, that Zn preferentially substitutes for Fe3+ as Zn2+ in the tetrahedral coordination, due to the affinity of Zn2+ for sp3 bonding with oxygen anions leaving all the ferric ions on the octahedral sites. In case of bulk Zn-doped magnetite, the total moment per unit cell increases, as the tetrahedral sites become occupied by the non-magnetic transition metal (Gorter, 1954). Such dopants no longer partially cancel the Fe moment in the octahedral coordination. For Zn doping the average moment of the octahedral Fe sites also slightly increases as charge neutrality requires that some of the octahedral Fe2+ convert to Fe3+. If Ga substitutes into the tetrahedral coordination as a Ga3+ ion (instead of Zn2+), it should produce a similar, though slightly reduced effect.Bulk (GaxFe(1-x))3O4 magnetic trends have not been fully studied, but Ga is typically present as a trivalent ion (Ga3+), so it is likely to be present in this valence state given the two options in the spinel structure. From simple crystal f lling arguments, the reduced ion radius of Ga3+ in comparison to Zn2+ suggests that the Ga dopant should more strongly prefer the tetrahedral coordinated site than Zn, allowing for a further investigation of the peculiar moment behavior. The doping of Ga as trivalent cation (Ga3+) in the tetrahedral conf guration causes the moment per iron atom of the particles to increase with increasing Ga concentration until 20% Ga, after which the nonmagnetic nature of Ga causes the moment to quickly fall to 0 in a manner similar to other dopant materials in bulk Fe3O4.Indium has been previously incorporated into spinel structures, including ferrites, especially concerning the potential utilization of this dopant (111In) as a radiotracer for biomedicinal use.

In this work superparamagnetic nanoparticles (SPMNPs) of magnetite and doped-magnetite with either gallium or indium were produced by the chemicalcoprecipitation method, in order to study the influence of doping metal on the magnetic and the optical properties of the produced magnetic nanoparticles.The structure of the produced magnetic nanoparticles was determined by using X-Ray Diffraction analysis (XRD), Scanning Electron Microscopy (SEM) and Vibrating Sample Magnetometry (VSM).

2. Materials and Methods

2.1 Synthesis of magnetic nanoparticles

The magnetic nanoparticles (MNPs) were prepared by chemical coprecipitation route, based on the procedure published elsewhere (Antipas et al., 2013; Giannouli, 2013), used as precursor materials for Fe3+ and Fe2+ the hydrated chloride salts of trivalent and bivalent iron, FeCl3·6H2O and FeCl2·4H2O, respectively. In brief, the precursor solutions of these iron salts were prepared by the addition of the proper quantities solid salts into an aquatic solution of hydrochloric acid (12 N). Finally, the as-prepared mixed aquatic solution of iron salts was added carefully into a preheated aquatic solution of NaOH (1.5 M) at 90°C, under continuous stirring and reflux and the temperature during the whole mixing process was kept in the range of 60-80^{0}C. The formation of a black precipitate (magnetite or/and maghemite) was done almost directly after the mixing process of salts with alkali solution. For the production of doped-magnetite a part of trivalent iron was substituted by trivalent gallium and indium ions. In these cases, the nitrate salts, Ca(NO3)3 and In(NO3)3, were used as precursor materials for Ga3+ and In3+, respectively. In any case, the molar ratio Fe2+ / Fe3+, Ga3+, In3+ must be ½.The doped-magnetite with Ga or In was produced by substitutingtrivalent gallium or indium for trivalent iron partially, by using various mixing ratios of Ga3+/Fe3+ and In3+/Fe3+ solutions, as shown in Table 1.

2.2 Characterization Techniques

X-Ray powder diffraction spectra for all the prepared samples of pure and doped magnetite were obtained in reflection (Bragg-Brentano geometry) by a BrukerD8 Focus diffractometer, fitted with a rotating Cu-anode (λ=1.5406 Å) at a power of 1.6 kW. The diffracted X-rays were collected after Ni-filtering on a scintillation counter.Scanning electron microscopy measurements were performed with the JEOL JSM 6380LV electron microscopeand the elemental analysis was performed with the X-Ray micro-analyzer (EDS) (Oxford INCA Energy 250).Vibrating Sample Magnetometry experiments were conducted on a VSM 155 Princeton Applied Research (2T). By using VSM, the magnetic properties of the prepared magnetic samples were investigated through the recording of the variation of magnetization of the vibrating sample against the applied magnetic field under constant temperature (20^{0}C) one the one hand and against the temperature, under a constant applied magnetic field (1T), on the other hand.

Table 1: The mixing ratios of Ga^{3+}/Fe^{3+} and In^{3+}/Fe^{3+} solutions used for the synthesis of nanosized pure and doped magnetite samples

Sample	$FeCl_3 \cdot 6H_2O$	$FeCl_2 \cdot 4H_2O$	$In(NO_3)_3$	$Ga(NO_3)_3$
2	1.23M → 8.6 g	0.6 M → 3.1 g	-	-
3	1 M → 6.9 g	0.6 M → 3.1 g	-	0.23 M →1.2 g
4	0.75 M → 5.2 g	0.6 M → 3.1 g	-	0.48 M → 2.6 g
5	0.5 M → 3.5 g	0.6 M → 3.1 g	-	0.73 M → 3.9 g
6	1 M →6.9 g	0.6 M → 3.1 g	0.23 M → 1.5 g	-
7	0.75 M → 5.2 g	0.6 M → 3.1 g	0.48 M → 3.1 g	-
8	0.5 M → 3.5 g	0.6 M → 3.1 g	0.73 M → 4.7 g	-

3. Results and Discussion

The structural characterization results of X-Ray Diffraction analysis for all the samples of produced magnetic nanoparticles (pure magnetite or/and doped with Ga^{3+} or In^{3+}) are represented below by Figures 1-3.

The comparison of Figures 1 and 2, which concern pure magnetite and Ga-doped magnetite, respectively, clearly shows two identical diffraction spectra. The absence of any other peak (e.g., $Ga \cdot (GaOH)_3$) than that of magnetite in Figure 2 further indicates the complete incorporation of Ga^{3+} into the spinel structure (e.g., $FeO \cdot (GaFe)_2O_3$). Contrary to this, doping of magnetite with In_{3+} led to the emergence of another peak except for magnetite, which is possibly concerns $In(OH)_3$ or $FeIn(OH)_6$, as Figure 3 indicates. These observations could be explained if consider the very similar ionic radius of trivalent iron (Fe^{3+}: 0.67 Å) and trivalent gallium (Ga^{3+}: 0.62 Å) on the one hand, which permits the complete incorporation of Ga^{3+} in magnetite structure instead of Fe^{3+} and the significant higher ionic radius of indium (In^{3+}: 0.8 Å) than of Fe^{3+} on the other hand, which does not permit the corresponding substitution of indium for ferric ions. Moreover, the experimental conditions used for indium and ferric/ferrous ions coprecipitation perhaps were not thermodynamically favourable for the incorporation of indium ions inside the spinel structure. A general observation from all the above XRD diffractograms is that all the prepared samples are nanosized ferrites.

The above results from XRD-analysis of the prepared magnetic samples were more confirmed by SEM-EDS analysis results of these samples, as they are depicted in the following Figures 4 and 5. Among the various Ga-ferrite samples prepared by using various mixing ratios for solutions of gallium and iron salts – see Table 1 – the sample prepared with most quantity of gallium gave the clearest SEM-image and it is that of Figure 5 (on the top). That fact further means that the higher quantity of gallium used the higher conductivity of the corresponding ferrite resulted.

The results of magnetic measurements for pure nanomagnetite as well for doped nanomagnetite samples are represented in Figures 6-8. A general observation from these Figures is that a phase-change is taking place at the temperature proximity of 200^0C. As one can see from Figure 7 concerning Ga-ferrite, there is observed a little Ga-ferrite-phase, which is disappeared just after cooling the sample. The same situation is recorded for all prepared Ga-doped magnetite samples (Ga-ferrite samples). Thus, if Ga-ferrites are going to be used in various applications, there is strictly demanded not to overcome the temperature of 200^0C.

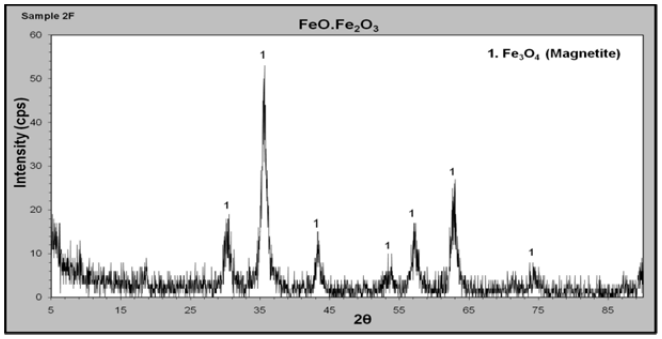

Figure 1: XRD diffractogram for pure magnetite samples ($FeO \cdot Fe_2O_3$).

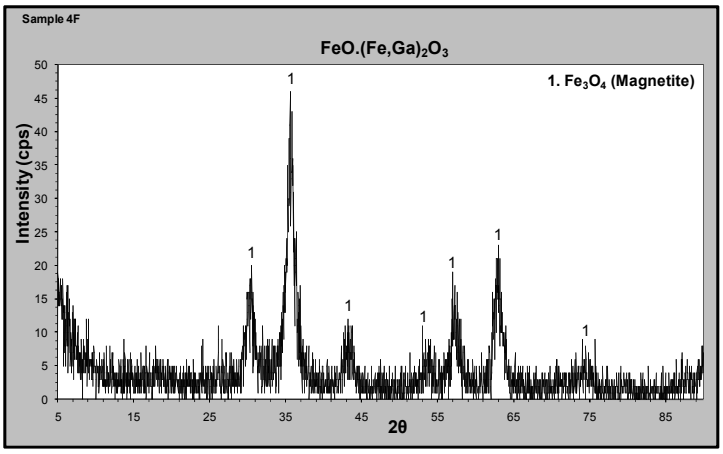

Figure 2: XRD diffractogram for Ga-doped magnetite samples ($FeO\cdot(Fe,Ga)_2O_3$).

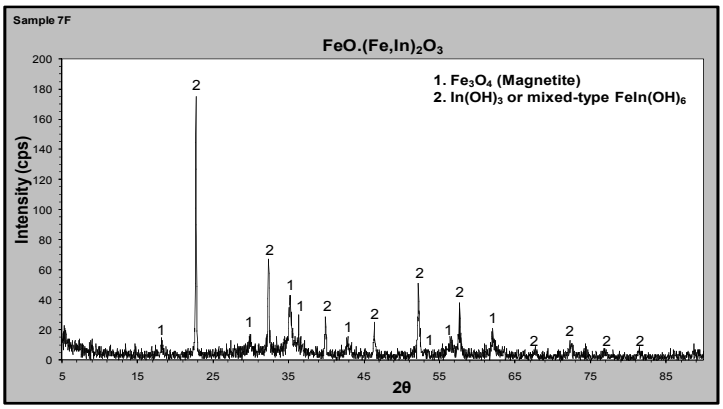

Figure 3: XRD diffractogram for In-doped magnetite samples ($FeO\cdot(Fe,In)_2O_3$).

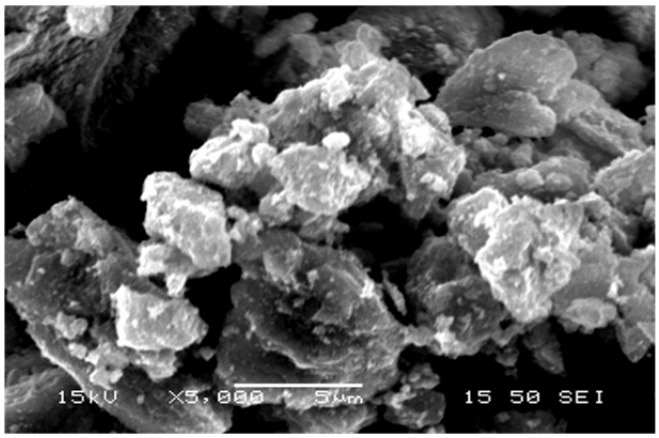

Figure 4: SEM image of pure magnetite sample.

In case of In-doped magnetite samples (In-ferrite samples) magnetic responses which are depicted in Figure 8, apart from ferrite-phase another phase is observed, which is disappeared just after cooling the sample. The last fact probably indicates that a quantity of In-dopant has been incorporated into the sublattice of the spinel crystal. In addition to this, the magnetization of the cooled material of In-doped sample is ~45 $A\cdot m^2\cdot kg^{-1}$, namely smaller than that of pure ferrite (pure magnetite – see Figure 6), which implies that after cooling the material is hematite.

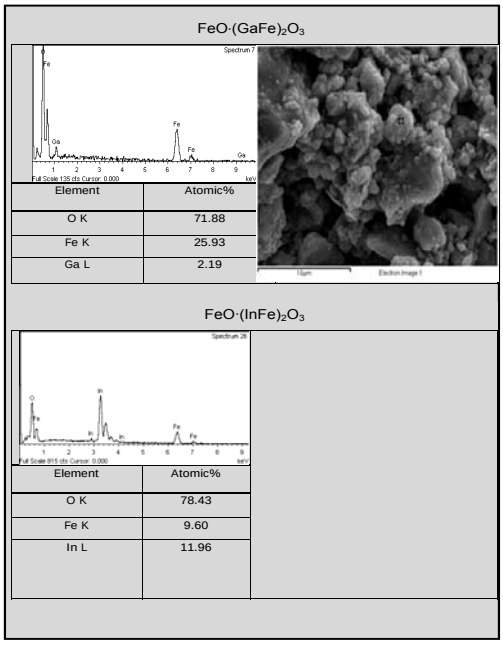

Figure 5: SEM images of doped with gallium(Ga) and indium(In)magnetite samples.

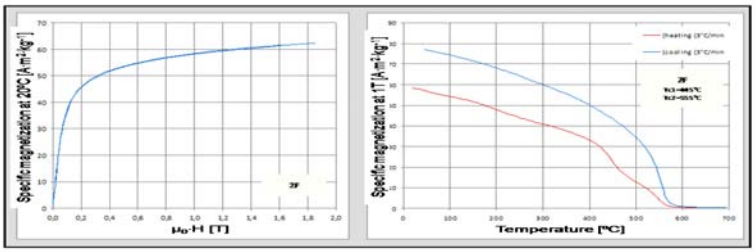

Figure 6: Magnetic measurements results for pure magnetite (Fe_3O_4) samples.

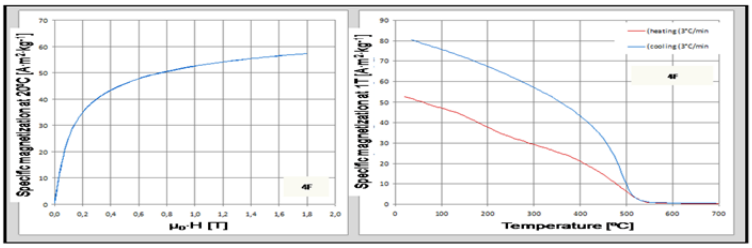

Figure 7: Magnetic measurements results for doped with gallium magnetite (Ga-ferrite) samples.

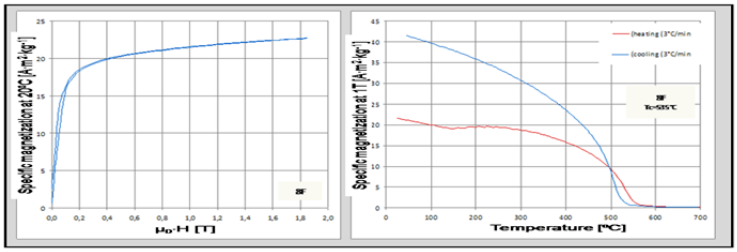

Figure 8: Magnetic measurements results for doped with gallium nanomagnetite (Ga-ferrite) samples.

4. Conclusions

In this work, the role of partial substitution of trivalent iron (Fe^{3+}: 0.67 Å) in spinel ferrites by the trivalent ion of gallium (Ga^{3+}: 0.62 Å) or indium (In^{3+}: 0.8 Å) on the magnetic and optical properties of magnetite was studied. A general result from the applied methodology is that all the synthesized samples are nanosized materials. Moreover, the ferrite produced by using the higher quantity of gallium was the most conductive Ga-ferrite material. Finally, the induced influences on the magnetic properties of magnetite by the use of gallium as dopant material, namely the increase in the magnetic anisotropy and the significant magnetic hardening (analytical simulations calculate a magnetic anisotropy 1 $MJ \cdot m^{-3}$) of Ga-ferrite, making Ga-doped magnetite nanoparticles smaller than 5 nm potential candidates for use as hard magnets. However, it should be noted that in applications of Ga-ferrites, the temperature limit of 200˜ C should not be overcome. On the other hand, the doping of magnetite with indium produces a ferrite material with changeable semiconductivity, due to the induced change in the energy gap (E_g) in the order of meV, making In-ferrites potential candidate materials for the control of reflection and/or absorption of electromagnetic radiation.

Acknowledgments

This work has received funding from the European Union's Horizon 2020 research and innovation programme FET-OPEN under grant agreement No 665318 - HELENIC-REF.

Reference

Antipas G.S.E., Statharas E., Tserotas P., Papadopoulos N., Hristoforou E., 2013, Experimental and First-Principles Characterization of Functionalized Magnetic Nanoparticles, Chem. Phys. Chem. 14, 1934-1942.

Chikazumi S., Taketomi S., Ukita M., Mizukami M., Miyajima H., Setogawa M., Kurihara Y., 1987, Physics of magnetic fluids, J. Magn. Magn. Mater. 65, 245-251.

Chistyakov A.V., Murzin V.Y., Gubanov M.A., Tsodikov M.V., 2013, Pd-Zn Containing Catalysts for Ethanol Conversion Towards Hydrocarbons, Chemical Engineering Transactions, 32, 619-624.

Deraz N.M., 2012, Effects of magnesia addition on structural, morphological and magnetic properties of nano-crystalline nickel ferrite system, Ceramics International 38, 511-516.

Giannouli C., 2013, Magnetite: Synthesis and Characterization, Key Eng. Mater. 2253 (2013) 460.

Gorter E.W., 1954, Saturation magnetization and crystal chemistry of ferrimagnetic oxides, Philips. Res. Rep., 9(4), 295-320.

Gupta A.K., Gupta M., 2005, Synthesis and surface engineering of iron oxide nanoparticles for biomedical applications, Biomaterials 26(18), 3995-4021.

Hyeon T., 2003, Chemical synthesis of magnetic nanoparticles, Chem. Commun. (Camb.) 21(8), 927-934.

Kodama T., Tabata M., Sano T., M. Tsuji, Y. Tamaura, 1995, XRD and Mössbauer Studies on Oxygen-Deficient Ni(II)-Bearing Ferrite with a High Reactivity for CO2 Decomposition to Carbon, J. Solid State Chem. 120, 64-69.

Mornet S., Vasseur S., Grasset F., Verveka P., Goglio G., Demourgues A., Portier J., Pollert E., Duguet E., 2006, Magnetic nanoparticle design for medical applications, Prog. Solid State Chem. 34, 237-247.

Nordhei C., Mathisen K., Safonova O., Wouter van Beek, Nicholson D.G., 2009, Decomposition of Carbon Dioxide at 500 °C over Reduced Iron, Cobalt, Nickel, and Zinc Ferrites: A Combined XANES−XRD Study J. Phys. Chem. C 113, 19568-19577.

Palma V., Ciambelli P., Meloni E., 2013, Catalyst Load Optimization for Microwave Susceptible Catalysed DPF, Chemical Engineering Transactions, 32, 799-804.

Peña M.A., Pierro J.L.G., 2001, Chemical structures and performance of perovskite oxides, Chem. Rev. 101(7), 1981-2017.

Ruzmanova Y., Ustundas M., Stoller M., Chianese A., 2013, Photocatalytic Treatment of Olive Mill Wastewater by N-doped Titanium Dioxide Nanoparticles under Visible Light, Chemical Engineering Transactions 32, 2233-2238.